

# Antenna Design and Channel Measurements for On-Body Communications at 60 GHz

X. Y. Wu\*, Y. Nechayev, P. S. Hall

\*xxw881@bham.ac.uk

*Electronic, Electrical and Computer Engineering, University of Birmingham  
Edgbaston, Birmingham, B15 2TT  
United Kingdom*

**Abstract**— On-body communication is of increasing interest for a number of applications, such as medical-sensor networks, emergency-service workers, and personal communications. This paper reviews 60 GHz on-body communication and its benefits and challenges. Two novel low profile high gain, end-fire wearable antennas are then described. Measurements with an experimental phantom and real human body are presented. Results show antennas achieve good performance close to a phantom. Shadowing effects and polarisation issues for on-body communications at 60 GHz are discussed.

## I. INTRODUCTION

The ever-growing miniaturization of electronic hardware and embedded systems, combined with recent developments in wearable communication technology, are leading to the creation of body area network (BAN) communication systems which refer to human-self and human-to-human networking with the use of wearable and implanted wireless sensors. It has abundant applications in personal healthcare, smart home, personal entertainment and identification systems, space exploration and military. Recently, there has been extensive research into on-body antennas and propagation at 2.45GHz and UWB bands. Studies on many related topics have been carried out, including wearable antenna design [1]-[3], on-body channel characterization [4],[5], the effect of human body presence on the link performance, on-body diversity [6],[7] etc. Although on-body communications have been advanced in recent years, many applications are still not well served by current standards and technology. In particular, there is no wireless solution currently for applications that require high levels of electromagnetic energy control, to minimise interference with other equipment and susceptibility to observation and jamming, coupled with high data rates. Security is now considered to be a paramount requirement for BANs, and uncertainties about it may even be holding back faster deployment. Security can mean that BANs may interfere with other systems, for example ISM band based medical sensor networks in hospitals will have to coexist with other equipment working in these bands. Also there is a fear the outside systems may be able to interfere with BANs, either to deny use or to insert false data; this is again a problem for medical sensor networks.

The band around 60 GHz seems to be promising solution to these applications because of its significant advantages for body area networks, in particular, small RF components and antennas, high free space losses and hence lower interference, visibility and susceptibility to interference, a wide available spectrum (57-64GHz) and high data rates. However, 60 GHz band also has some difficult challenges such as high cost.

Besides, due to more directional antennas, the shadowing effect from the human body may be more significant and it makes non-line-of-sight communication very difficult. In this paper, we present two novel Yagi-Uda antennas for 60 GHz on-body communications, namely the printed Yagi-Uda array and the substrate integrated waveguide (SIW) Yagi-Uda antenna. Measurements using these antennas with phantoms and on a real human body are demonstrated.

## II. ON-BODY ANTENNA REQUIREMENTS

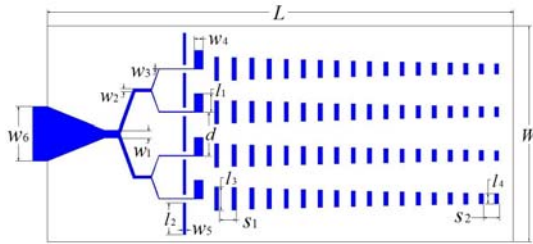
Commonly, wearable antennas should be low profile, light weight, and ideally conformal to the body surface. However, due to 60 GHz propagation characteristics, there are some additional requirements. First, because of high path loss at 60 GHz, high antenna gain is needed to offset channel loss. According to path loss calculations, at least 10 dBi gain is required at both the transmitter and the receiver for a line of sight path of human body dimensions. And second, for this kind of scenario, the maximum of the radiation pattern should be tangential to the body surface to maximize coupling between bodyworn devices. Previous studies showed that a monopole antenna gives very good results for on-body applications at lower frequencies [6], but it cannot provide for the high gain required in the 60 GHz band. Therefore, an end-fire pattern is required. Such high gain antennas also lead to better security, as minimize the amount of energy radiated away from the body, thus giving good BAN to BAN and BAN to fixed base station isolation. For the aforementioned reasons, the Yagi-Uda antennas have been chosen as strong candidates because of their good compromise in terms of size and gain performance compared to some other end-fire antennas such as tapered slot antennas.

## III. PRINTED YAIGI-UDA ANTENNA

Variants of the printed Yagi antenna have been introduced in [9]. Based on these, a single printed Yagi antenna has been designed with a driven dipole, 18 directors and one reflector on both sides of a 0.127 mm thick RT/Duroid 5880 substrate ( $\epsilon_r=2.2$ ,  $\tan \delta=0.0009$ ). In order to increase the antenna gain even further an array of four Yagi antennas has been designed. Fig. 1 shows this array and its dimensions. One half of each driven dipole is placed on one side of the dielectric substrate and the other half on the opposite side. Symmetrical parallel lines are used as a feeding structure which is printed on both sides of the substrate. Due to the 180° phase difference between the currents on the upper line and the lower line of this feed, the sidelobe level degradation due to feed radiation

is significantly reduced, compared to, for example, coplanar strip feeding. The substrate used is thin compared to the wavelength so the vertical displacement of the dipole arms results in an insignificant effect on the radiation pattern. The spacing and length of directors are decreased gradually according to a geometric series in order to achieve higher gain and lower sidelobe level.

A four-way power divider is designed to equally distribute power to each single antenna. This power divider is also patterned on both sides of the substrate. At the end of the power divider, a parallel line to microstrip line transition is introduced using a tapered ground plane. The center-to-center spacing between two adjacent antennas in the array,  $d$ , is 3mm to maximize the array gain and minimize the side-lobe level.



$L=32.6$   $I_1=1.298$   $I_2=2.2$   $I_3=1.65$   $I_4=0.6898$   $W=15$   $W_1=0.5068$   
 $W_2=0.204$   $W_3=0.048$   $W_4=0.6$   $W_5=0.2$   $W_6=3.7592$   $d=3$   
 $S_1=1.175$   $S_2=1.1376$

Fig. 1 Bottom view of the printed Yagi array with its dimensions (mm)

Due to equipment setup, waveguide interface was used in the measurements. A 2-step ridged waveguide to microstrip transition is adopted for measurement because of broad bandwidth, good match and wide range of available impedances. The transition and Yagi array on an experimental phantom of fresh meat are shown in Fig. 2. The distance between the antenna and the phantom was 5mm. Fig. 3 shows the simulated and measured reflection coefficient. A 5 GHz bandwidth from 55 GHz to 60 GHz is achieved. Although there is a frequency shift due, we assume, to a fabrication error, reasonable agreement can be seen. It can also be observed that the phantom does not significantly affect the reflection coefficient. Fig. 4 shows the radiation patterns of the array. The red line shows simulated pattern. The line with triangle markers and the line with square markers show the measured co-polarised patterns without and with the experimental phantom, respectively. The dash line shows cross-polarised pattern without the phantom. The measured gains with and without the phantom are 15.0 and 15.7 dBi, respectively. However, the radiation pattern normal to the phantom that is, in the H plane is somewhat affected. The cross-polarisation levels are relatively high in both the planes due primarily to the radiation from the open aperture of the transition.

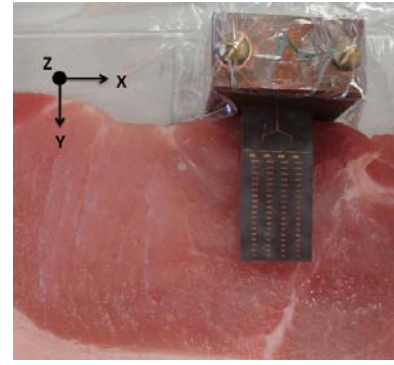


Fig. 2 The printed Yagi array on the experimental phantom

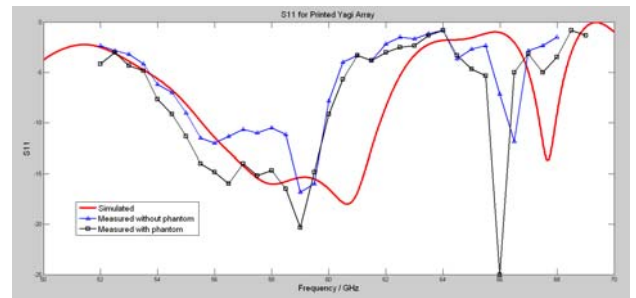


Fig. 3 Reflection coefficient of the printed Yagi array

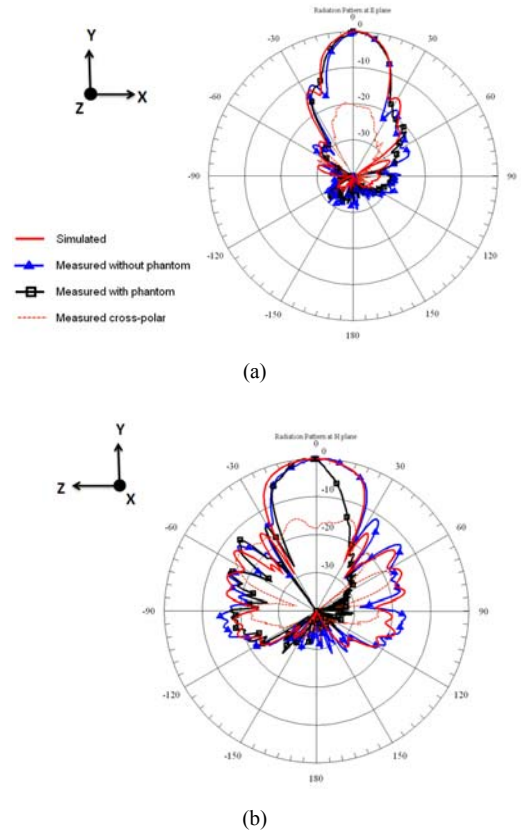
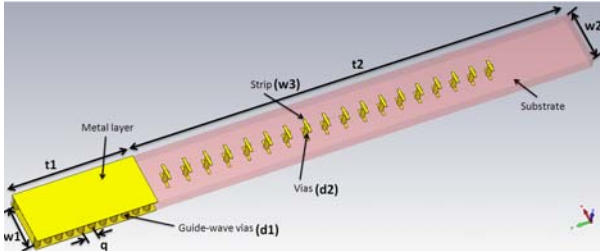


Fig. 4 Radiation pattern of the printed Yagi array at 60GHz: (a) E plane (b) H plane

#### IV. SUBSTRATE INTEGRATED WAVEGUIDE YAGI ANTENNA

Recently, substrate integrated waveguide (SIW) technology has been demonstrated as a promising candidate for millimeter wave integrated circuits and systems for the next decade. Based on planar dielectric substrates with top and bottom metal layers perforated with metallic vias, SIW structures offer a compact, low loss, flexible, and cost-effective solution for integrating active circuits, passive components and radiating elements on the substrate [10].

The schematic and geometry of the SIW Yagi antenna is shown in Fig. 5. On the the left side of the antenna is a planar guide-wave structure, where two periodic rows of metallic vias are applied to form the sidewalls of the waveguide. The substrate used here is RT/Duroid 5880 substrate ( $\epsilon_r=2.2$ ,  $\tan \delta=0.0009$ ), with thickness of 0.787 mm. The width of the SIW is  $w_1=2.6$  mm. The diameter and spacing of the vias are  $d_1=0.4$  mm and  $q=0.65$  mm, respectively.



$t_1=7.15$ mm,  $t_2=26.2$ mm,  $d_1=0.4$ mm,  $d_2=0.3$ mm,  $q=0.65$ mm,  $w_1=2.6$ mm,  $w_2=3.2$ mm,  $w_3=0.15$ mm

Fig. 5 Schematic of SIW Yagi-Uda antenna

Another row of vias with a diameter of 0.3 mm is also inserted into the substrate, to act as the directors of the Yagi-Uda antenna. The vias are loaded at the top and the bottom with printed strips to make sure the equivalent length of the directors is half wavelength. The width of strips,  $w_3$ , is 0.15mm. The spacing between the adjacent strips is gradually decreased from 1.2375 mm to 1.0537mm by a factor of 0.98. The lengths of strips are reduced according to a geometric series in order to achieve higher gain and lower sidelobe level. As high currents flow in the vias of the parasites, the radiated polarisation is normal to the substrate, unlike the printed Yagi array described before, which is polarised in the plane parallel to the substrate.

A multi-step transition between the SIW and the WR 15 standard air-filled waveguide is used for measurement. It uses a three-step quarter-wavelength impedance transformer. The measurement results with and without an experimental phantom are presented below. The reflection coefficient of the SIW Yagi antenna is shown in Fig. 6. Results show a good agreement between the simulation and the measurement with and without the experimental phantom, which indicates that the phantom does not significantly affect the reflection

coefficient. Both the simulated and measured radiation patterns in E and H plane at 60 GHz are shown in Fig. 7. The measured maximum gains without and with the phantom are 12.5 dBi and 10 dBi, respectively. This 2.5dB difference is probably because the polarisation of this antenna is normal to the experimental phantom which also affects somewhat the pattern in E plane.

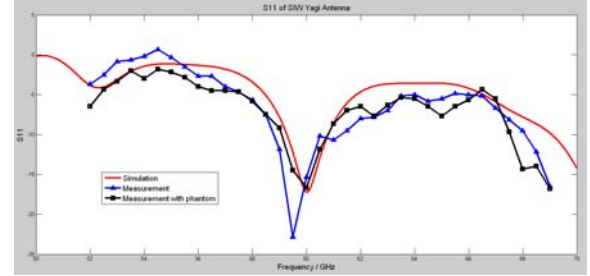


Fig. 6 Reflection coefficient of the substrate integrated waveguide Yagi antenna

#### V. ON-BODY MEASUREMENTS AND POLARISATION ISSUES

Previous studies showed that for many channels, an antenna polarised normally to the body's surface gives the best path gain at 2.45 GHz [5]. In this paper, an investigation of this issue at 60 GHz is presented. We use three pairs of different kinds of antennas, namely 20-dB gain standard horns, SIW Yagi antennas and printed Yagi arrays, mounted on the human body to investigate on-body channels at 60 GHz. The measurement system consists of the signal generator, frequency multiplier, power amplifier, antennas, low noise amplifier, mixer and spectrum analyser. The block diagram of the system is shown in Fig. 8. The measurement setup is shown in Fig. 9. The receiver was fixed on the front side of the calf and the transmitter was moved along the body surface, with the transmitter and receiver pointing approximately at each other. The Tx-Rx separation was changed from 2 cm to 70 cm, and the noise floor was at -75dB. Each scenario was measured five times. Fig. 10 shows the measured path gain along the body surface using the three tested antenna pairs. Provided the antenna gain differences are taken into account, the results indicate that the polarisation does not considerably affect the path gain for this link at 60 GHz.

Some non-line-of-sight links on the body at 60 GHz were also measured, but no signal was received in those cases because of the shadowing by the human body which is rather severe at these frequencies and can create big difficulties in supporting communications over non-line-of-sight links on human body. However, reconfigurable antennas could probably overcome this problem, by switching to non-obscured ray paths. For example, a belt-to-back link could make use of the floor or ceiling reflections.

Fig. 10 Path gain results with different antenna pairs

## VI. CONCLUSIONS

A printed Yagi-Uda antenna array and a substrate integrated waveguide Yagi-Uda antenna working at around 60 GHz have been proposed for use in on-body communication channels. Antenna performances with and without the experimental phantom have been investigated. The results show that they can achieve greater than 10 dBi gain, end-fire radiation pattern, and wide impedance bandwidth even in close proximity of the phantom, confirming their suitability for on-body applications. Measurements with the real human body have also been conducted. The results indicate that the polarization does not significantly affect the path gain and that establishing on-body non-line-of-sight communication links at 60GHz can be challenging. A possible solution to this problem is proposed.

## REFERENCES

- [1] Conway G. A. and Scanlon W. G., "Antenna for Over-Body-Surface Communication at 2.45 GHz", *IEEE Transactions on Antenna and Propagation*, vol.57 no. 4, April 2009, p844-p855
- [2] Rais, N.H.M.; Soh, P.J.; Malek, F.; Ahmad, S.; Hashim, N.B.M.; Hall, P.S.; "A Review of Wearable Antenna", *Antennas & Propagation Conference, 2009. LAPC 2009. Loughborough*, Page(s): 225 - 228
- [3] Haga, N.; Saito, K.; Takahashi, M.; Ito, K.; "Characteristics of Cavity Slot Antenna for Body-Area Networks", *Antennas and Propagation, IEEE Transactions on Volume 57, Issue 4, Part 1, April 2009* Page(s):837 - 843
- [4] Hu, Z.H.; Gallo, M.; Bai, Q.; Nechayev, Y.I.; Hall, P.S.; Bozzetti, M.; "Measurements and Simulations for On-Body Antenna Design and Propagation Studies, Antennas and Propagation", 2007. *EuCAP 2007. The Second European Conference on 11-16 Nov. 2007* Page(s):1 - 7
- [5] Hall, P.S.; Yang Hao; Nechayev, Y.I.; Alomalny, A.; Constantinou, C.C.; Parini, C.; Kamarudin, M.R.; Salim, T.Z.; Hee, D.T.M.; Dubrovka, R.; Owadally, A.S.; Wei Song; Serra, A.; Nepa, P.; Gallo, M.; Bozzetti, M.; *Antennas and Propagation for On-Body Communication Systems, Antennas and Propagation Magazine, IEEE Volume 49, Issue 3, June 2007* Page(s):41 - 58
- [6] I Khan, P.S. Hall, A.A Serra, A.R. Guraliuc, P. Nepa, "Diversity Performance Analysis for On-body Communication Channels at 2.45 GHz", *IEEE Transactions on Antennas and Propagation*, Vol. 57, No. 4, April 2009.
- [7] I. Khan, P.S. Hall, "Multiple Antenna Reception at 5.8 and 10 GHz for Body-Centric Wireless Communication Channels", *IEEE Transactions on Antennas and Propagation*, Vol. 57. No. 1, January 2009.
- [8] Daniels, R.C.; Heath, R.W.; "60 GHz wireless communications: emerging requirements and design recommendations", *IEEE Vehicular Technology Magazine*, Volume: 2, Issue: 3, 2007, Page(s): 41 - 50
- [9] Grajek, P.R.; Schoenlinner, B.; Rebeiz, G.M.; "A 24-GHz high-gain Yagi-Uda antenna array", *IEEE Transactions on Antennas and Propagation*, Vol. 52, Issue: 5, 2004, Page(s): 1257 - 1261
- [10] M. Bozzi, L. Perregrini, K. Wu, P. Arcioni, "Current and Future Research Trends in Substrate Integrated Waveguide Technology", *Radio Engineering*, vol. 18, no. 2, June 2009

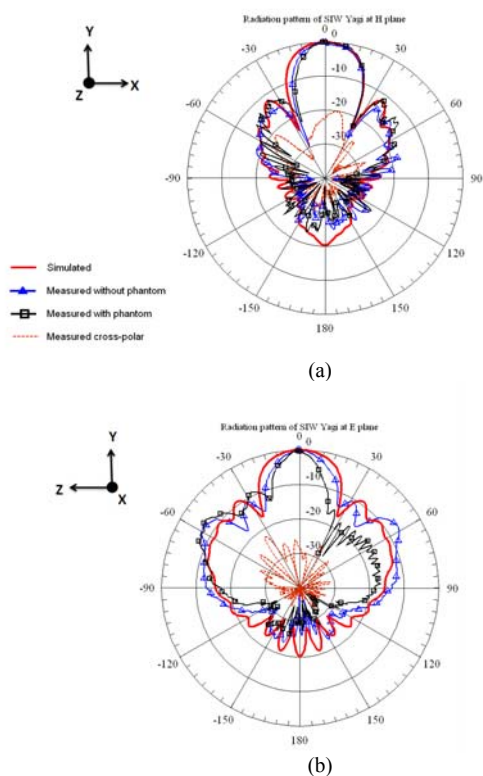


Fig. 7 Radiation pattern of the printed Yagi array at 60GHz: (a) E plane (b) H plane

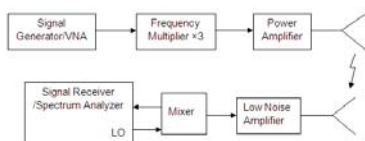


Fig. 8 Block diagram for 60 GHz on-body measurement system



Fig. 9 On-body measurement setup

